J. Eukaryot. Microbiol., 52(1), 2005 pp. 31–37
© 2005 by the Society of Protozoologists

Development and Molecular Characterisation of the Microsporidian *Schroedera airthreyi* n. sp. in a Freshwater Bryozoan *Plumatella* sp. (Bryozoa: Phylactolaemata)

DAVID J. MORRIS,[a] REBECCA S. TERRY[b] and ALEXANDRA ADAMS[a]

[a]*Institute of Aquaculture, University of Stirling, Stirling, FK9 4LA, UK and*
[b]*School of Biology, University of Leeds, Leeds, LS2 9JT, UK*

ABSTRACT. The development of a new species of microsporidian, infecting a freshwater *Plumatellid* bryozoan, is described. The small-subunit rDNA, internal transcribed spacer region (ITS), and partial large-subunit rDNA genes were sequenced. Phylogenetic analysis demonstrated that the parasite clustered with *Schroedera plumatellae*. However, while there were morphological affinities with this species, significant differences were also observed. The infection initially appeared as a roughening of the peritoneum lining the metacoelom of the bryozoan. This roughening resolved into meront-infected syncytia, composed of interconnected cells of the body wall that detached to float in the coleomic cavity. Spores were observed to develop within these syncytia. All stages of development were diplokaryotic in contrast to *S. plumatellae*, which has a distinct monokaryotic merogony preceding sporogony. The infection was pathogenic to the host. Direct bryozoan–bryozoan transmission was not observed. We propose to name the microsporidian *Schroedera aithreyi* n. sp.

Key Words. *Bacillidium*, Mrazekiidae, Pseudonosematidae.

A number of new species of microsporidia have recently been described infecting a range of freshwater bryozoa. The microsporidian species are from four different genera: *Pseudonosema cristatellae*, *Trichonosema pectinatellae*, *Bryonosema plumatellae*, *Bryonosema tuftyi*, and *Schroedera plumatellae* (Canning Okamura, and Curry 1997; Canning et al. 2002; Morris and Adams 2002). A further species, *Nosema bryozoides*, has also been described from the bryozoan *Plumatella fungosa* (Korotneff 1892). However, because of lack of data, it has been proposed to move this parasite species to the holding genus *Microsporidium* until it can be more accurately described (Canning et al. 2002).

To date, all of the microsporidia that infect bryozoa produce diplokaryotic spores that resemble those of the genus *Nosema*. Phylogenetic analyses using the small subunit (SSU) rDNA gene sequences derived from the recently described species have demonstrated that they are not related to *Nosema* spp. but cluster around sequences derived for *Bacillidium* spp. and *Janacekia debaisieuxi*, parasites infecting oligochaetes and dipteran hosts, respectively (Canning et al. 2002; Morris and Adams 2002). However, there are striking morphological differences between the spores of the bryozoan infecting microsporidia and those of *Bacillidium* spp. and *J. debaisieuxi*. Notably, the large bacilliform spores of the genus *Bacillidium* possess a modified polar filament known as a manubrium, while the smaller pyriform spores of the bryozoan-infecting species possess an isofilar polar filament. In addition, *J. debaisieuxi* produce monokaryotic spores as opposed to the diplokaryotic spores produced by both the bryozoan parasites and *Bacillidium* spp. As such, the relationship between these parasites was speculated upon. For the description of *Schroedera plumatellae* Morris and Adams (2002) assigned a new sister genus to the *Bacillidium* within the family Mrazekiidae, while the microsporidian genera *Trichonosema*, *Bryonosema*, and *Pseudonosema* were ascribed to a new family, Pseudonosematidae by Canning et al. (2002). When the Pseudonosematidae was proposed, it was recognised that *Janacekia* and *Bacillidium* could not form part of this family. The expectation being, that the inclusion of future microsporidian rDNA sequences would improve the phylogeny of the group and demonstrate that the genera were not closely related (Canning et al. 2002).

The recent elucidation of a SSU rDNA gene sequence for *Bacillidium vesiculoformis* has further strengthened a phylogenetic relationship between the Pseudonosematidae and the genus *Bacillidium* (Morris et al. 2005). Observations on the development of *Bacillidum* spp. have suggested similarities with the bryozoan-infecting microsporidia. In particular, these include the presence of additional exosporal material, diplokaryotic sporogony, and a preceding monokaryotic merogony for *S. plumatellae* and *B. vesiculoformis* (Morris and Adams 2002; Morris et al. 2005).

Here we describe the phylogeny and development of a new species of the genus *Schroedera* and discuss its relationship with other members of this intriguing group of microsporidian parasites.

MATERIALS AND METHODS

Collection and culture of colony. A bryozoan colony with adherent bark was removed from a branch at the southern end of Airthrey Loch, University of Stirling, in May 2001. The colony was glued into the centre of a 9-cm plastic Petri dish using a cyanacrylate adhesive and all macro-invertebrates removed. The colony was cultured following the protocol of Morris, Morris, and Adams (2002), and observed daily using an inverted microscope for signs of parasite infection within it.

Transmission electron microscopy. Portions of infected colony were placed in Karnovsky's fixative for 4 h and rinsed in 0.1 M cacodylate buffer (pH 7.2) overnight. They were then post-fixed in osmium tetroxide for 1 h, passed through an acetone to alcohol series, and embedded in Spurr's resin. Semi-thin sections (1 μm) were cut and stained using methylene blue–fuchsin for light microscopy. Ultra-thin (gold/silver) sections were cut, mounted on formvar-coated grids, and stained with lead citrate/uranyl acetate. They were viewed using a Philips 201 electron microscope at 80 kV.

Molecular characterisation. A portion of the infected colony was removed from the Petri dish, and the DNA extracted using a magnetic separation kit following the manufacturer's protocol (Abgene, Cambridge, UK). The SSU, internal transcribed spacer region (ITS), and partial large -unit subunit (LSU) rDNA were amplified from infected tissue, and sequenced using a range of microsporidian specific primers: V1f (Weiss et al. 1994), 18sf, 530r (Baker et al. 1995), 530f, 228r, 580r (Vossbrinck et al. 1993), 964r (Terry et al. 2003), and HA3Bf, HG4f, HG4r (Gatehouse and Malone 1998). Amplifications were carried out in 50-μl volume using a Robocycler 96 gradient polymerase chain reaction (PCR) machine (Stratagene Europe, Amsterdam, the Netherlands). Each individual reaction contained 10 pmol of each primer, 0.2 mM of each dNTP, 1.5-mM $MgCl_2$, and 1.25 U of Go *Taq* polymerase (Promega, Southampton, UK). The amplification program consisted of 95 °C for 5 min, followed by 40 cycles of 95 °C for 50 s, 50 °C for 70 s, and 72 °C for 90 s. Amplification was completed with a final elongation step of 72 °C for 10 min. PCR products

Corresponding Author: D. Morris—Telephone number: +44 1786 467912; FAX number: +44 1786 473122; E-mail: d.j.morris@stir.ac.uk

were visualised on 1.5% agarose gels using ethidium bromide staining. PCR products were then cleaned for sequencing using a QIAquick gel extraction kit (Qiagen, Inc., Sussex, UK) and sequenced at the Natural History Museum, London.

Phylogenetic analysis. A homology search was performed using the FASTA program (European Bioinformatics Institute, Cambridge, UK). The sequence was then aligned, using Bioedit (Hall 2001), with 20 other microsporidian SSUrDNA sequences from GenBank as follows: *Amblyospora connecticus* (AF25685); *Bacillidium* sp. (AF104087); *Bacillidium vesiculoformis* (AJ581995); *Brachiola algerae* (AF069063); *Bryonosema plumatellae* (AF484690); *Edhazardia aedis* (AF027684); *Encephalitozoon cuniculi* (L17072); *Glugea anomala* (AF104084); *Janacekia debaisieuxi* (AJ252950); *Loma acerinae* (AJ252951); *Nosema bombycis* (L39111); *Oligosporidium occidentalis* (AF495379); *Pleistophora typicalis* (AF104080); *Pseudonosema cristatellae* (AF484694); *Schroedera plumatellae* (AY135024); *Encephalitozoon intestinalis* (L39113); *Thelohania solenopsae* (AF134205); *Trichonosema pectinatellae* (AF484695); *Vairimorpha necatrix* (Y00266); *Visvesvaria acridophagus* (AF024658). Sequences were rooted against two zygomycete fungal sequences, *Basidiobolus ranarum* (D29946) and *Mycotypha microspora* (AF157148). Only those portions that could be unambiguously aligned were used in the phylogenetic analysis. Parsimony, neighbour joining, and maximum likelihood analyses were performed using PAUP*4.0[b10] (Swofford 2002). A modification of the GTR+I+G substitution model (four γ classes) was generated by deleting factors from the model that caused a reduction of the log likelihood value (ln L) of no more than one. A heuristic search was employed with random stepwise addition (10 replicates) and TBR branch swapping. Nodal support of the maximum likelihood analysis was assessed by bootstrap analysis (100 replicates).

RESULTS

Bryozoa culture and nature of parasitised colony. After 2 days in culture the colony started to grow onto the surface of the Petri dish. Eight days later, a portion of the colony appeared to be parasitised when viewed under an inverted microscope. As the infection progressed the infected colony became pale white in colour. Viewed under a dissecting microscope, the extent of the infection could be traced to zooids on the opposite side of the bark. The infection was limited to a single colony that was identified as having an observable common metacoel. This colony was intertwined with at least one other bryozoan colony that was not infected.

Examination of microsporidian development. The infection initially appeared as numerous cell groups, forming on the peritoneum that lined the metacoel of the bryozoan giving it a roughened appearance (Fig. 1). The cell groups would gradually become extruded from the peritoneum, remaining attached by cytoplasmic extensions. At this time, within the body wall of the bryozoan, diplokaryotic meronts could be observed (Fig. 2). Eventually, the groups of cells would become detached from the peritoneum to float in the metacoel of the bryozoan where the motion of the coelomic fluid would transport them around the colony. The cytoplasmic extensions remained on the cell groups as they were transported and were observed as being static, entwined with one another to form fixed points. As the infection progressed the entire peritoneum of the colony appeared to be forming these cell groups.

Initiation of statoblast formation (i.e. bryozoan asexual propagules) was observed during the early stages of the infection. However, these never matured and they gradually became reabsorbed into the funiculus of the zooids. In contrast, neighbouring uninfected colonies produced numerous mature statoblasts (Fig. 1).

Some of the cell groups, free in the metacoel, were released from the bryozoan through the lophophore. When this happened, the lophophore would retract and the cell groups would be ejected from between its tentacles, presumably through the vestibular pore, which is normally associated with statoblast release. The zooids of the neighbouring colony/ies were observed to actively ingest these cell groups. However, successful direct transmission of the infection was not noted.

Examination of the ejected cell groups demonstrated that they were parasitised and appeared to be at different stages of development. The simplest stage observed was an enlarged single cell containing two diplokaryotic meronts and a prominent host cell nucleus (Fig. 3). The majority of cell groups were arranged as groups of three to 18 cells. Usually an enlarged central cell, infected with diplokaryotic meronts, was surrounded by variable numbers of attached host cells. The nuclei of all of the host cells in the group appearing enlarged with prominent nucleoli. The cytoplasm of the attached cells was granular nearest to the infected cell and lucent furthest away. The cytoplasmic extensions observed within the bryozoan were only evident on a few cell groups as extensions formed from the host cells attached to the infected cell (Fig. 4). As the infected cell increased in size, the attached cells merged into the central cell, thus forming a multi-nucleated syncytium (Fig. 5). Some of these syncytia were observed to contain individual microsporidian spores (Fig. 6).

Within the bryozoan, the increasing numbers of syncytia and infected cell groups had a detrimental effect on the host. Notably, the lophophores gradually decreased in size, deforming the bryozoan (Fig. 7). The syncytia accumulated at the base of the reduced lophophore and became more rounded, filling with spores. The cytoplasm of the syncytia became reduced as the spores developed, eventually forming packets of spores, contained within a plasma membrane (Fig. 8). A small number of these spore packets were released by the lophophore and contained variable numbers of uniform, ovoid spores that tapered to one end, measuring 8.7 μm in length by 5.8 μm in diam. (Fig. 9). However, in the majority of cases the packets increased in number at the base of the lophophore. The zooid eventually died with masses of spores filling the end of the metacoel.

Ultrastructural features of cell groups. The earliest stages of parasite development noted were infected cells associated with the

Fig. **1–9.** Light microscopy of *Schroedera airthreyi* n. sp. **1.** Bryozoan colony growing on surface of Petri dish. Clusters of cells forming along the peritoneum (arrowheads), giving it a roughened appearance, with immature statoblasts indicated by arrow. Neighbouring zooids develop mature statoblasts. S, statoblast. Phase contrast. Scale bar = 500 μm. **2.** Infected bryozoan demonstrating diplokaryotic meronts within the body wall (arrow). Forming syncytia are visible within the metacoel of the bryozoan (*). Phase contrast. Scale bar = 15 μm. **3.** Single cell containing two meronts, ejected from the colony. In upper right is a portion of a syncytium also ejected from the colony. Phase contrast. Scale bar = 15 μm. **4.** Syncytia ejected from colony. The syncytia are composed of an infected central cell, containing meronts, and numerous attached cells with prominent nuclei. Cytoplasmic extensions can be observed on the attached cells. Phase contrast. Scale bar = 15 μm. **5.** Large syncytium containing numerous meronts and host cell nuclei. Few adherent cells remain. Phase contrast. Scale bar = 20 μm. **6.** Spores within ejected syncytium (arrow). Bright field. Scale bar = 10 μm. **7.** Reduced bryozoan lophophore in the infected colony. The inside of this portion of the colony appears opaque because of the large number of spores collecting within it. Phase contrast. Scale bar = 500 μm. **8.** Reduced syncytia filled with mature spores floating within the metacoel of the bryozoan. Phase contrast. Scale bar = 90 μm. **9.** Mature spores. Scale bar = 10 μm.

peritoneum of the bryozoan. Here elongate cells, filled with numerous diplokaryotic meronts were adjacent to the peritoneum of the bryozoan (Fig. 10). The diplokaryon occupied the majority of the meront's cytoplasm. The infected cell was connected to neighbouring host cells by fine cytoplasmic bridges and tight junctions. The nuclei of these neighbouring host cells were irregular in shape and had prominent nucleoli. The transition of these cells to the stages observed within the metacoel was not observed.

Infected cells were observed throughout the metacoel and also within the mesoceol of the lophophore (Fig. 11). The surfaces of these infected cells were covered in fine cytoplasmic extensions, and had a granular cytoplasm containing irregular nuclei and

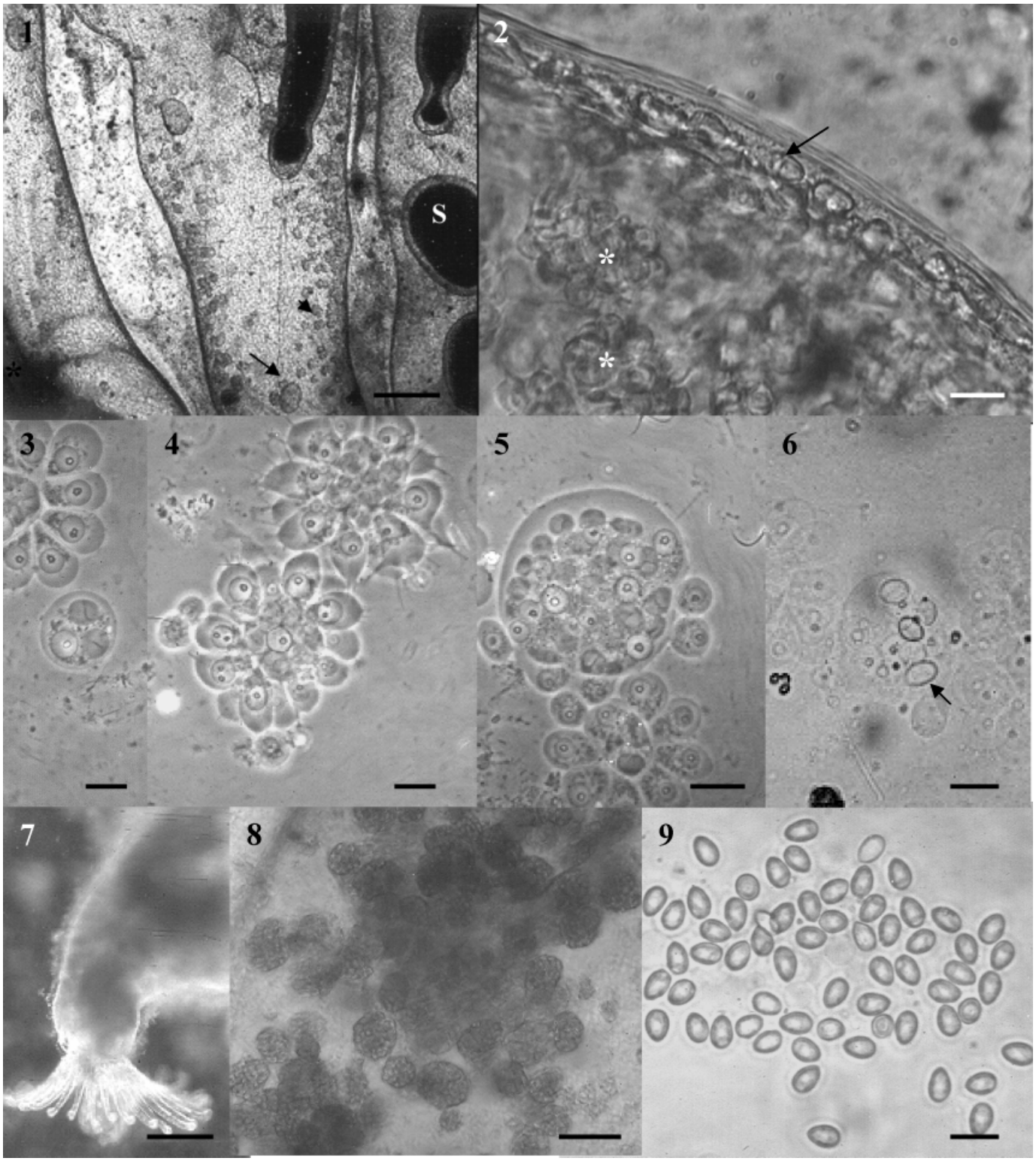

numerous mitochondria. They contained large numbers of diplokaryotic meronts, sporonts, and developing spores (Fig. 12). The uninfected host cells that were associated with the infected cell also had an irregular nucleus with prominent nucleolus and numerous mitochondria. They were held in position by the surrounding uninfected cells enclosing a portion of the attached cell's

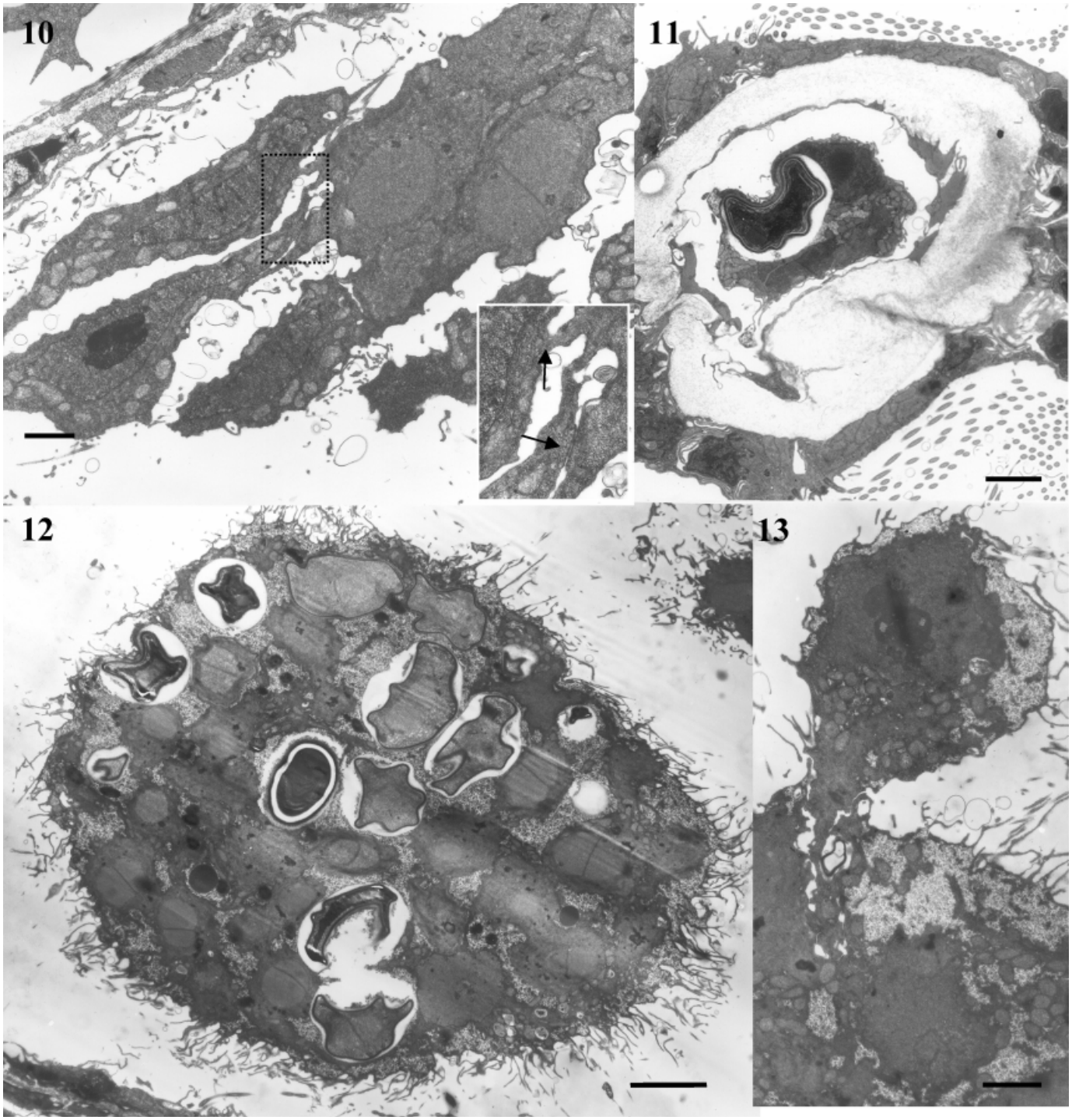

Fig. **10–13.** Ultrastructure of presporogonic stages of *Schroedera aithreyi* n. sp. **10.** Wall of the bryozoan with infected cells containing diplokaryotic meronts overlying the peritoneum. The insert highlights the attachment of the infected cell to neighbouring host cells either directly or through tight junctions (arrows). Scale bar = 2 μm. **11.** Syncytium containing sporoblast within the mesoceol of lophophore tentacle. Scale bar = 2 μm. **12.** Infected cell within the metacoel of an infected bryozoan. Meronts, sporonts, and sporoblasts are all present within the cell, which has numerous cytoplasmic extensions. Scale bar = 5 μm. **13.** Host cell attached to infected syncytium. The nucleus of this cell contains a prominent nucleolus and mitochondria arranged towards the infected cell. The surface of the attached cell is covered in cytoplasmic extensions as is the surface of the syncytium. Scale bar = 2 μm.

cytoplasm (Fig. 13). Meronts were observed dividing within the syncytium by binary division (Fig. 14).

Sporogony. The transition of merogony to sporogony was initiated with areas of the meront's plasmalemma becoming dense together with an increase in the amount of endoplasmic reticulum (Fig. 15). On these dense areas of plasma membrane, material was deposited, although it could not be determined whether this was derived from the developing sporont or the host cell (Fig. 16). Eventually the plasma membrane of the whole parasite became covered by material. At this stage of development many sporonts appeared crescent-shaped (Fig. 17). Several of the sporonts also appeared to be dividing by binary division (Fig. 18). The cell surface of the individual sporonts then became thickened and dense. With this surface thickening, structures associated with sporogony became visible within the spore. The first of these was the anchoring apparatus observed as a dense body. As the sporont developed, the cytoplasm became increasingly lucent. The anchoring apparatus developed at the anterior end of the sporont while a polar tube and posterior vacuole developed at the posterior end. The diplokaryon became increasingly difficult to differentiate from the cytoplasm (Fig. 19).

Spores. Fixation of the spores was very poor and none were observed that were properly fixed. The following description is made from a composite of partially fixed spores. The spores were pyriform with a centrally located diplokaryon and 37–38 turns of the polar filament arranged in one to four rows around the periphery of the spore (Fig. 20). Two dense bodies were noted towards the posterior of the spores, together with homogenous, granular posterior vacuole. The polar filaments were composed of five concentric layers of material. Although, fixation of the polaroplast was generally poor, it appeared to be bell-shaped and of a very dense lamellar construction (Fig. 21). The anchoring disc had a dense cap and was surrounded by the polar sac that tapered over the surface polaroplast (Fig. 22). The wall of the spores was composed of three layers, a dense endospore, surrounded by an exospore of two distinct layers, a dense layer with an overlying granular layer. The exospore became noticeably reduced over the anchoring disc of the spore.

Very occasionally, aberrant spores were noted. These were oval and superficially appeared mature, but either lacked a polaroplast and anchoring apparatus or if present, these structures appeared abnormal, being composed solely of stacked lamellae.

Phylogenetic analysis. The complete SSU, ITS, and partial LSU rDNA of the parasite were 1615 bp in length (GC content 41.92%) and have been deposited in GenBank (AJ749819). The FASTA search revealed that the sequence had 87% identity with *S. plumatellae*, 84% identity to *B. plumatellae*, and 77% identity to *B. tuftyi*, all parasites of Bryozoa. Eighty-one per cent identity was seen between *S. plumatellae* and *B. plumatellae*. The close identity with these bryozoan parasites was also seen in the phylogenetic trees with parsimony, neighbour joining, and maximum likelihood all giving the same overall topology (Fig. 23, parsimony and neighbour joining data not shown). *Bryonosema tuftyi* was not included in this analysis because of the short sequence length available.

DISCUSSION

This microsporidian is differentiated from other bryozoan infecting microsporidia by its development, ultrastructural morphology, and its SSUrDNA gene sequence. The notable distinguishing morphological feature of the spore is the relatively large number of turns of the polar filament (37–38 compared with the maximum of 33 for all of the other known bryozoan-infecting microsporidia).

Phylogenetic analysis demonstrated that this isolate clusters closest with *S. plumatellae* and *B. plumatellae*. The spore wall of all of these species consists of a bilayered exospore, which has in addition to a dense layer and a layer of granular material (Canning et al. 2002; Morris and Adams 2002). The spore wall of *B. tuftyi* also includes this granular material on the exospore. The relative length of the *B. tuftyi* SSUrDNA gene sequence available precluded it from our phylogenetic analysis, although sequence alignment analysis suggested that *B. tuftyi* was distinct from this isolate with only 77% sequence identity. The genera *Schroedera* and *Bryonosema* were reported concurrently in the literature and morphological similarities between these genera suggest that they may be congeneric. However, sequence identity and phylogenetic analysis clearly supports the division of these species into two distinct genera. The new isolate clusters closest to *S. plumatellae*, therefore warranting its inclusion within the genus *Schroedera*. While there are morphological and developmental similarities between *S. plumatellae* and our new isolate significant developmental differences also exist. Both species induce the formation of syncytial masses of host cells. In our new isolate, these are derived from cells of the body wall while in *S. plumatellae* they are from spermatogonic cells and spermatids. Both types of syncytia possess numerous cytoplasmic extensions on their surface. However, the major developmental difference between the two species is that sporogony of *S. plumatellae* is preceded by a monokaryotic merogony while for our new isolate diplokaryotic merogony precedes sporogony. Therefore, given these notable and significant differences, we propose to name this new isolate, *Schroedera airthreyi* n. sp.

Description of species

Systematic position. Phylum Microsporidia, Class Dihaplophasea, Order Dissociodihaplophasida, Family Mrazekiidae, Genus *Schroedera*

Name. Schroedera airthreyi n. sp.

Type host. Plumatella sp, (Bryozoa, Phylactolaemata)

Type locality. Southern end of Airthrey Loch, University of Stirling campus, National grid reference NS 804963. Latitude 56°8.8′N, longitude 3°55.3′W.

Infected cell locality. Cells of body wall that detaches to float in the metacoel.

Type material. Hapantotype material has been deposited in the collection of the Natural History Museum, London. This material comprises embedded blocks of bryozoa containing the early stages of parasite development (registration number 2004:8:27:1) and later stages of development including spores and sporonts (registration numbers 2004:8:27:2 and 2004:8:27:3).

Etymology. The specific name relates to the name of the type locality.

Description. Parasite induces the formation of syncytia composed of cells from the host's body wall. Diplokaryotic in all stages of development. Merogony by binary division, disporoblastic, sporoblasts also dividing by binary division. All stages develop in direct contact with syncytial cytoplasm.

Description of spores. Fresh spores ovoid, tapering anteriorly, 8.7 ± 0.3 μm in length, 5.8 ± 0.4 μm in width ($n = 20$). Diplokaryotic centrally located with 37–38 turns of the isofilar polar filament arranged in one to two rows around the periphery of the spore. Dense spheroids present towards posterior of spore. Exospore consists of two layers, a dense layer surrounded by a granular layer.

The life cycles of members of both the Mrazekiidae and Pseudonosematidae remain unknown. Transmission studies have indicated that direct transmission does not occur, with at least one alternate host required in the life cycle (Morris and Adams 2002;

Morris et al. 2005). An alternative host may also be necessary for the life cycle of *S. airthreyi* as the neighbouring bryozoa did not appear to become infected. The expulsion of developing syncytia from the infected colony may be an attempt at reducing the infection by the bryozoan rather than as a dispersal mechanism for the parasite as few spores were observed in this material.

While it may be considered that the genus *Schroedera* has many affinities with the Pseudonosematidae, the close phyloge-

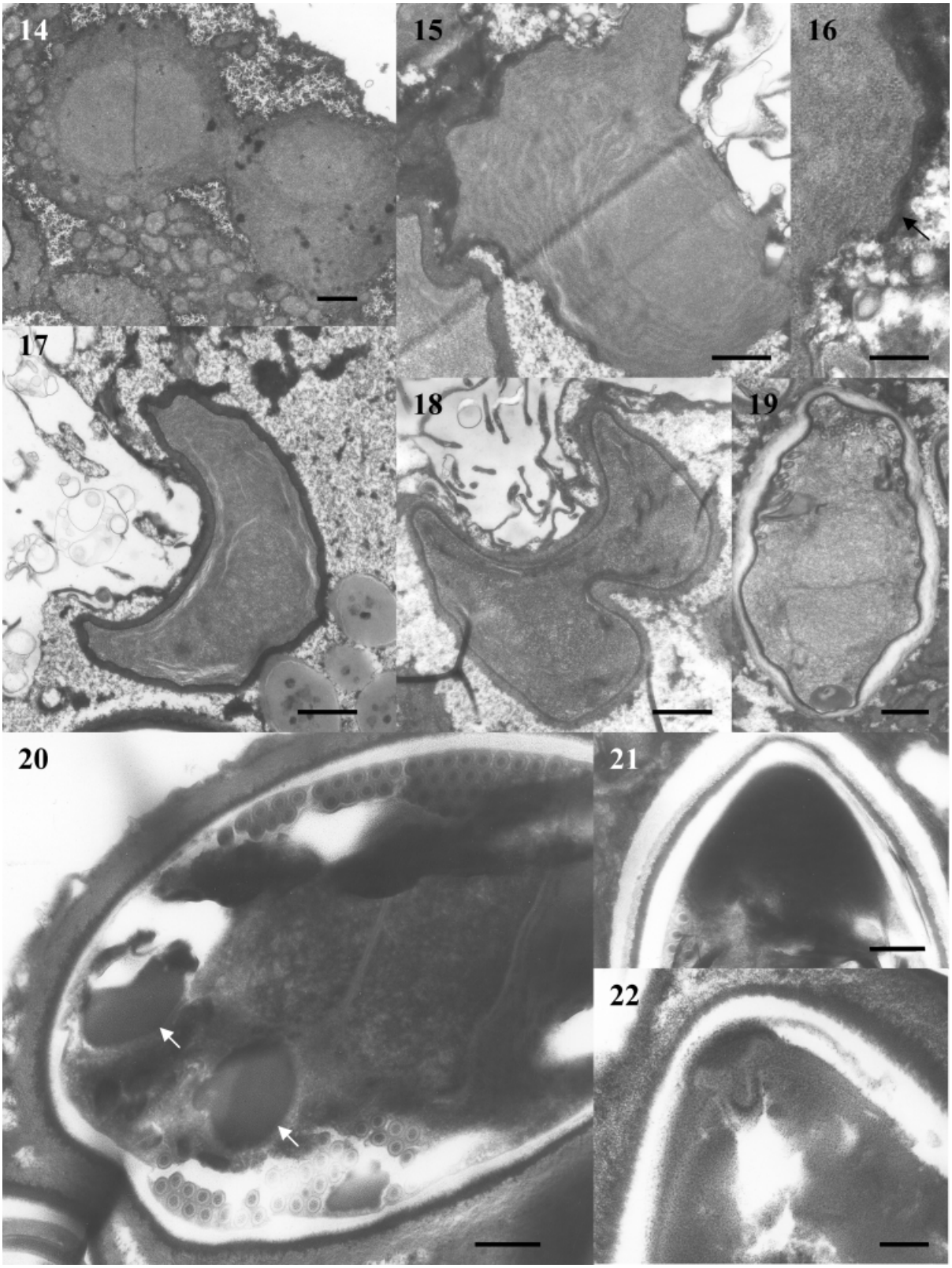

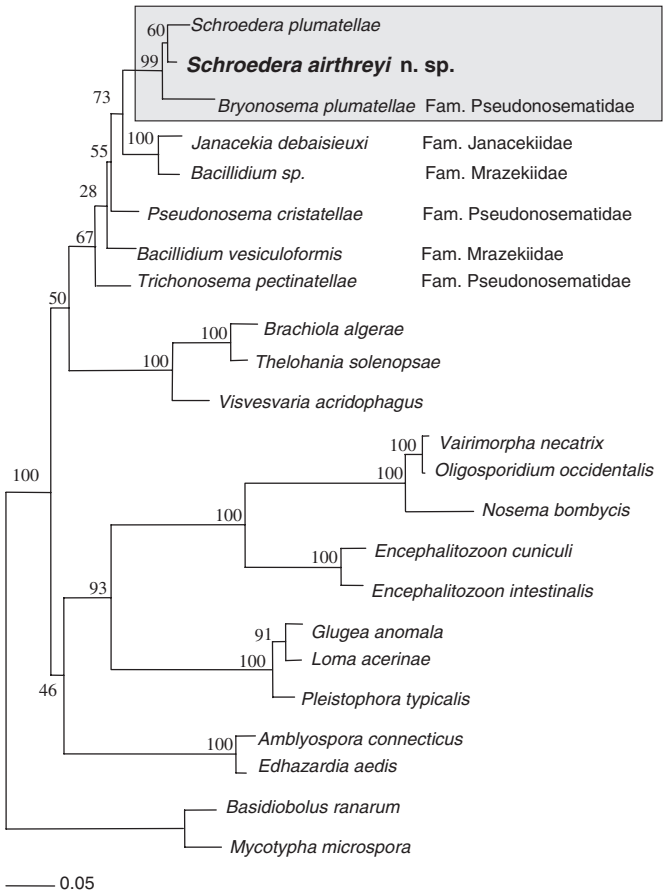

Fig. **23.** Microsporidian phylogenetic tree based on small subunit rDNA using maximum likelihood analysis. *Schroedera airthreyi* n. sp. forms a clade with *Schroedera plumatellae* and *Bryonosema plumatellae* (highlighted box). The bootstrap values (100 replicates) on the tree represent the percentage of bootstrap replicates that gave the topology.

netic association between members of the families Mrazekiidae and Pseudonosematidae indicates that the two groups are interrelated. Microsporidia with indirect life cycles can have different spore types that relate to the different hosts (Andreadis 1985; Sweeney, Hazard, and Graham 1988). As such, it is likely that members of the Mrazekiidae and Pseudonosematidae form alternate parts in the life cycles of the same parasites, in which case precedence dictates that the Pseudonosematidae become a junior synonym of the Mrazekiidae. It is expected that future phylogenetic analysis of further *Bacillidium* spp. and *Janacekia* spp. will resolve many of the questions relating to the biology and relationships between these parasites and clarify the higher taxonomy of the genus *Schroedera*.

ACKNOWLEDGMENTS

The authors would like to thank the Department of Environment and Rural Affairs (project FC1111) and the Natural Environment Research Council (NER/A/S/1999/60040) for funding these studies. We would also like to thank Mr. Linton Brown for his assistance with electron microscopy and Dr. Judith E. Smith for comments on the manuscript.

LITERATURE CITED

Andreadis, T. G. 1985. Life-cycle, epizootiology, and horizontal transmission of *Amblyospora* (Microspora: Amblyosporidae) in a univoltine mosquito, *Aedes stimulans*. *J. Invert. Pathol.*, **46**:31–46.

Baker, M. D., Vossbrinck, C. R., Didier, E. S., Maddox, J. V. & Shadduck, J. A. 1995. Small subunit ribosomal DNA phylogeny of various microsporidia with emphasis on AIDS-related forms. *J. Eukaryot. Microbiol.*, **42**:564–570.

Canning, E. U., Okamura, B. & Curry, A. 1997. A new microsporidium, *Nosema cristatellae* n. sp. in the bryozoan *Cristatella mucedo* (Bryozoa, Phylactolaemata). *J. Invert. Pathol.*, **70**:177–183.

Canning, E. U., Refardt, D., Vossbrinck, C. R., Okamura, B. & Curry, A. 2002. New diplokaryotic microsporidia (Phylum Microsporidia) from freshwater bryozoans (Bryozoa, Phylactolaemata). *Eur. J. Protistol.*, **38**:247–265.

Gatehouse, H. S. & Malone, L. A. 1998. The ribosomal RNA gene region of *Nosema apis* (Microspora): DNA sequence for small and large subunit rRNA genes and evidence of a large tandem repeat unit size. *J. Invert. Pathol.*, **71**:97–105.

Hall, T. 2001. Bioedit: Biological sequence alignment editor for Windows 95/98/NT Edition 5.0.9. *http://www.mbio.ncsu.edu/BioEdit/bioedit.html*

Korotneff, A. 1892. *Myxosporidium bryozoides*. *Zeitsch. Wiss. Zool.*, **53**:591–596.

Morris, D. J. & Adams, A. 2002. Development of *Schroedera plumatellae* gen. n., sp. n. (Microsporidia) in *Plumatella fungosa* (Bryozoa: Phylactolaemata). *Acta Protozool.*, **41**:383–396.

Morris, D. J., Morris, D. C. & Adams, A. 2002. Development and release of a malacosporean (Myxozoa) from *Plumatella repens* (Bryozoa: Phylactolaemata). *Folia Parasitol.*, **49**:25–34.

Morris, D. J., Terry, R. S., Ferguson, K. D., Smith, J. & Adams, A. (2005). Ultrastructural and molecular characterization of *Bacillidium vesiculoformis* n. sp. (Microspora: Mrazekiidae) in the freshwater oligochaete *Nais simplex* (Oligochaeta: Naididae). Parasitology, **30**:31–45.

Sweeney, A. W., Hazard, E. I. & Graham, M. F. 1988. Life-cycle of *Amblyospora dyxenoides* sp. nov. in the mosquito *Culex annulirostris* and the copepod *Mesocylops albicans*. *J. Invert. Pathol.*, **51**:46–57.

Swofford, D. L. 2002. PAUP*. Phylogenetic Analysis Using Parsimony (*and other methods), v. 4.0^{b10}. Sinauer Associates, Sunderland, MA.

Terry, R. S., MacNeil, C., Dick, J. T. A., Smith, J. E. & Dunn, A. M. 2003. Resolution of a taxonomic conundrum: and ultrastructural and molecular description of the life cycle of *Pleistophora mulleri* (Pfeiffer 1895; Georgevitch, 1929). *J. Eukaryot. Microbiol.*, **50**:266–273.

Vossbrinck, C. R., Baker, M. D., Didier, E. S., Debrunner-Vossbrinck, B. A. & Shadduck, J. A. 1993. Ribosomal DNA sequences of *Encephalitozoon hellem* and *Encephalitozoon cuniculi*: species identification and phylogenetic construction. *J. Eukaryot. Microbiol.*, **40**:354–362.

Weiss, L. M., Zhu, X., Cali, A., Tanowitz, H. B. & Wittner, M. 1994. Utility of microsporidian rRNA in diagnosis and phylogeny: a review. *Folia Parasitol.*, **41**:81–90.

Received: 06/25/04; accepted: 10/12/04

Fig. **14–22.** Ultrastructure during sporogenesis of *Schroedera airthreyi* n. sp. **14.** Meronts undergoing binary division within syncytium. Scale bar = 1 μm. **15.** Transition of meront to sporont. Material starts to form on the surface of the parasite, which contains large amounts of endoplasmic reticulum. Scale bar = 500 nm. **16.** Detail of sporont, demonstrating localised nature of material forming on the plasma membrane, indicated by arrow. Scale bar = 200 nm. **17.** Cell surface of sporont becomes totally enclosed with material, becoming dense. The diplokaryon becomes increasingly indistinct. Scale bar = 1 μm. **18.** Apparent disporoblastic division of sporonts. Scale bar = 1 μm. **19.** Developing sporoblast with increasing amounts of dense material forming on the plasma membrane. Note the anchoring apparatus developing at the anterior of the sporoblast while the polar filament develops at the posterior end. The diplokaryon is centrally positioned. Scale bar = 1 μm. **20.** Mature spore. Centrally located diplokaryon with two dense, posterior, spheroids (arrows) and 38 turns of the polar filament. Bar = 500 nm. **21.** Dense, bell-shaped, polaroplast of mature spore. Scale bar = 400 nm. **22.** Anterior of spore with the anchoring disc covered by a dense polar cap while the polar sac extends around the apex of the spore surrounding the dense polaroplast. Scale bar = 200 nm.